Inorganic Chemistry
Communication
pubs.acs.org/IC

Fast Detection of Water and Organic Molecules by a Change of Color in an Iron(II) Microporous Spin-Crossover Coordination Polymer

Francisco J. Muñoz-Lara,[†] Ana B. Gaspar,[†] M. Carmen Muñoz,[‡] Andrey B. Lysenko,[§] Konstantin V. Domasevitch,[§] and José Antonio Real*,[†]

[†]Institut de Ciència Molecular/Departament de Química Inorgànica, Universitat de València, c/Catedrático José Beltrán Martínez 2, 46980 Paterna, València, Spain

[‡]Departament de Física Aplicada, Universitat Politècnica de València, Camí de Vera s/n, 46022 València, Spain

[§]Inorganic Chemistry Department, National Taras Shevchenko University of Kyiv, Kyiv 01033, Ukraine

Supporting Information

ABSTRACT: Here we present a novel three-dimensional iron(II) spin-crossover porous coordination polymer based on the bis(1,2,4-triazol-4-yl)adamantane (tr_2ad) ligand and the $[Au(CN)_2]^-$ metalloligand anions with the formula $\{Fe_3(tr_2ad)_4[Au(CN)_2)]_2\}[Au(CN)_2]_4·G$. The sorption/desorption of guest molecules, water, and five/six-membered-ring organic molecules is easily detectable because the guest-free and -loaded frameworks present drastically distinct coloration and spin-state configurations.

Sensory and memory functions are important in the development of functional porous coordination polymers (PCPs).[1] The sorption/desorption of guest molecules in PCPs can be monitored following a change in a solid-state property of the framework like magnetism,[2] luminescence,[3] conductivity,[4] or charge transport.[5]

In iron(II) spin-crossover[6] (SCO)-PCPs, the sorption/desorption of guest molecules may drastically influence the electronic ground state of the iron(II) nodes or may not have any effect. It depends on the chemical nature and size of the guest molecules that occupy the pores. Iron(II) SCO building blocks present labile electronic configurations switchable between the high-spin (HS) and low-spin (LS) states in response to external stimuli (temperature, pressure, light, or absorption/desorption of an analyte). In the HS and LS states, the iron(II) SCO centers reveal differences in magnetism, optical properties, dielectric constant, color, and structure. This switch can be performed for cooperative spin transitions (STs) within the hysteresis loop based on the first-order hysteretic ST, which confers to the material a memory function.[7]

Detection of the sorption/desorption of guest molecules in a framework can be done by monitoring the magnetic and optical outputs (temperature dependence of the magnetic susceptibility and/or by a change of color at a given temperature). In principle, a fingerprint in the form of a magnetic response pattern may be attainable for distinct analytes.

Two distinct types of three-dimensional (3D) SCO-PCPs have been synthesized in the last decades: on the one hand, frameworks where the iron(II) nodes are connected exclusively through flexible organic linkers, $[Fe(L)(NCS)_2]·G$ [L = 1,2-di-4-pyridylethylene (dpe; trans isomer),[8] 4,4′-azopyridine (azpy),[9] and DL-1,2-bis(4′-pyridyl)-1,2-ethanediol (bped)[10]] among others; on the other hand, frameworks where rigid $[M^{II}(CN)_4]^{2-}$ metalloligand anions and organic linkers bridge the metal centers. This last type of framework is referred to as a Hofmann-like SCO-PCP generically formulated as $\{Fe(L)[M(CN)_4]\}·G$ [L = pyrazine (pz),[11−13] azpy,[14] 4,4′-bis(pyridyl)-acetylene (bpac),[15] and dpe;[16] M^{II} = Ni, Pd, and Pt]. The SCO properties in all of these materials are tightly related to the chemical nature and size of the adsorbed guest molecules. Noteworthy are the results obtained from the SCO-PCPs $\{Fe(pz)[M(CN)_4]\}$ because the frameworks can allow reversible control of the magnetic and optical outputs through chemical response at room temperature.[10,11]

All SCO-PCPs described above are based on bis-monodentate pyridine-type organic connectors and NCS^- or $[M(CN)_4]^{2-}$ coordinating anions. Here we present a novel 3D iron(II) SCO-PCP based on the bis(1,2,4-triazol-4-yl)adamantane (tr_2ad) ligand[17] (Scheme 1) and the $[Au(CN)_2]^-$ metalloligand anions with the formula $\{Fe_3(tr_2ad)_4[Au(CN)_2]_2\}[Au(CN)_2]_4·8H_2O$ (**1**). Compound **1** was synthesized by slow diffusion in multiarm-shaped vessels (see the Supporting Information, SI). Hexagonal pink single crystals suitable for X-ray determination were obtained after 6 weeks. The crystal structure of **1** was solved at 120 K in the monoclinic *C*2/*m* space group.

Scheme 1. Molecular Structure of tr_2ad

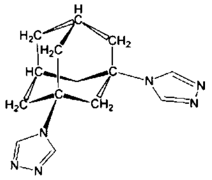

Relevant crystallographic data and bond lengths and angles are gathered in STable1 in the SI. There are two crystallographically distinct iron(II) sites labeled Fe1 and Fe2 (Figure 1, top). Both present an axially distorted octahedral coordination sphere consisting of six nitrogen atoms. The average Fe−N

Received: October 18, 2012
Published: December 4, 2012

dx.doi.org/10.1021/ic302287w | *Inorg. Chem.* 2012, 51, 13078−13080

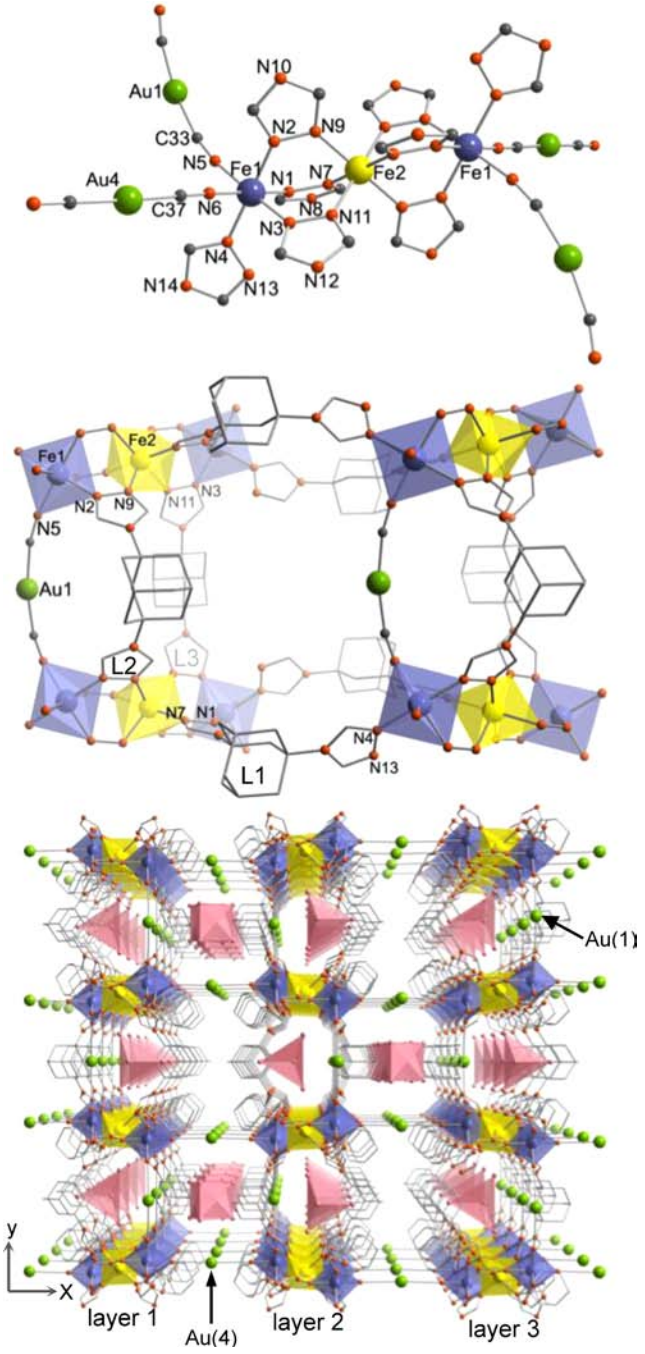

Figure 1. Top: Simplified view of the coordination spheres around the iron(II) atoms in **1** with the corresponding atom numbering. Middle: Projection of a fragment of the guest-free framework in the *xy* plane. Bottom: Projection in the *xy* plane of the guest-loaded framework. Color code: N, orange; C, gray; Fe, yellow and blue octahedra; O(H_2O), magenta tetrahedra and rhombic pseudocubic prisms; Au1 and Au4, green.

bond lengths [1.94(4) Å (Fe1) and 1.98(4) Å (Fe2)] are consistent with the LS state of the iron(II) ion, in agreement with the reported magnetic data (vide infra). Fe1 is coordinated to four different triazole rings belonging to three crystallographically distinct tr$_2$ad ligands labeled L1 with donor atoms (N1−N7−N4−N13), L2 (N2−N9), and L3 (N11−N3) and two distinct $[Au(CN)_2]^-$ anions (Au1 and Au4), which are in cis conformation (Figure 1, top and middle). The Fe2 site, coordinated to six triazole rings, lies in an inversion center. The Fe1 and Fe2 sites are triply bridged by three triazole rings, thereby forming Fe1−Fe2−Fe1 triads. The distance Fe1−Fe2 in the triad is 3.6438(8) Å. These triads are connected along the [001] direction by the L1 ligand, while along the [010] direction, the triads are connected through the $[Au1(CN)_2^-]$ anion and the tr$_2$ad ligands L2 and L3 (Figure 1, middle). The Fe···Fe distances through the organic bridge are in the range 10−13 Å, while they are slightly shorter through the $[Au(CN)_2^-]$ bridges (in the range 9−10 Å). This particular arrangement, mediated by the tr$_2$ad ligand and $[Au1(CN)_2^-]$ anions, leads to infinite layers lying in the *yz* plane. These layers stack along the [100] direction and are linked to each other by the $[Au4(CN)_2^-]$ anion through the Fe1 atoms (Figure 1, bottom). There are three additional different crystallographic $[Au(CN)_2^-]$ centers. $[Au2(CN)_2^-]$, $[Au3(CN)_2^-]$, and $[Au5(CN)_2^-]$ are not coordinated to the iron(II) metal centers. The $[Au2(CN)_2^-]$ and $[Au3(CN)_2^-]$ groups are situated parallel to the coordinated $[Au4(CN)_2^-]$ and $[Au1(CN)_2^-]$ anions, respectively, and show aurophilic interactions with Au···Au distances in a range on the order of 3.1−3.2 Å. The $[Au5(CN)_2^-]$ anions are sited in the channels delimited by the tr$_2$ad ligands running along the [100] direction with approximate dimensions of 8.2 × 8.2 Å^2 (see the SI). The guest water molecules fill in the remaining cavities not occupied by $[Au5(CN)_2]^-$ groups. Interestingly, they interact with each other through strong hydrogen bonds (2.7−2.9 Å), defining tetrahedral and rhombic pseudocubic prisms.

The magnetic susceptibility measurements indicate that **1** is diamagnetic in the temperature range of 2−300 K. Both Fe1 and Fe2 centers adopt the LS state. Thermogravimetric analysis (TGA) demonstrated that above 325 K the compound loses the guest water molecules (see the SI). The desorption of water takes place in two different steps, each one involving around four water molecules, and ends up around 400 K. Decomposition of the framework occurs at ca. 580 K. The water molecules can be reversibly sorbed/desorbed while crystallinity is maintained. Complete transformation of **1** into the dehydrated compound $\{Fe_3(tr_2ad)_4[Au(CN)_2]_2\}[Au(CN)_2]_4$ (**2**) is accomplished at 400 K. The sorption/desorption of water is easily detectable by the change of coloration that accompanies the transformation of **1** (pink) into **2** (light brown) (Figure 2).

The magnetic properties of the dehydrated compound **2** are depicted in Figure 2 in the form of $\chi_M T$ versus T (χ_M is the molar magnetic susceptibility and T the temperature). At 400 K, $\chi_M T$ approaches the value of 9 cm^3 K mol^{-1}; this value is slightly lower than that expected for the three iron(II) centers

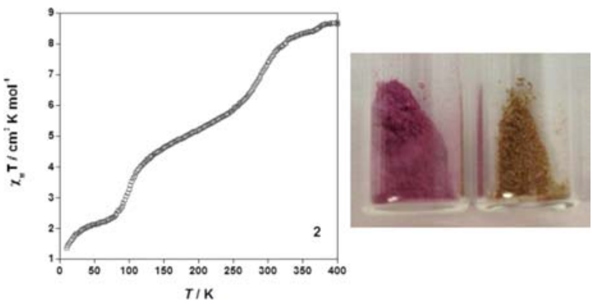

Figure 2. (Left) Magnetic properties of **2** in the form of $\chi_M T$ versus T. (Right) Coloration of the guest-loaded frameworks **1** and **3**−**6** (pink) and guest-free framework **2** (light brown).

in the HS state [between 3.2 and 3.6 cm^3 K mol^{-1} per iron(II) atom]. This reflects the existence of a small fraction of iron(II) centers in the LS state. Upon lowering of the temperature, $\chi_M T$ experiences a decrease to ca. 6 cm^3 K mol^{-1} at 250 K because of ST to the LS state of approximately one-third of the iron(II) ions. Below this temperature, the magnetic susceptibility decreases smoothly. Further lowering of the temperature shows an abrupt decrease of $\chi_M T$ between 120 and 90 K to attain a value of ca. 2.20 cm^3 K mol^{-1}, which indicates that more than two-thirds of the iron(II) centers underwent ST to the LS state. Below this temperature, ST is kinetically blocked and the observed decrease of $\chi_M T$ is ascribed to the zero-field splitting of the iron(II) ions that remain in the HS state. The thermal dependence of $\chi_M T$ in the warming mode coincides with that of the cooling mode. Taking into account the average Fe−N bond lengths, the high- and low-temperature steps could be ascribed to the Fe2 and Fe1 sites, respectively.

The guest water molecules in **1** can partially be replaced by furan, toluene, thiophene, or pyrrole (G), leading to frameworks with the following composition: $\{Fe_3(tr_2ad)_4[Au(CN)_2]_2\}[Au(CN)_2]_4 \cdot nH_2O \cdot qG$ [n = 5, q = 1, and G = furan (**3**); n = 2, q = 0.5, and G = toluene (**4**); n = 5, q = 2, and G = thiophene (**5**); n = 5, q = 2, and G = pyrrole (**6**); see the SI]. These polymers are obtained when the guest molecules are present during the crystallization process or by exposition of **2** to vapors of G in an open atmosphere. TGA−mass spectroscopy (MS) experiments performed on **3**−**6** have proven the presence of these organic guest molecules (see the SI). Powder X-ray diffraction (PXRD) patterns for **3**−**6** were recorded at 293 K (see the SI). Compounds **3**−**6** have very similar profiles, with most of the significant peaks located between 2θ = 5 and 15°. From these PXRD profiles and taking into account the analytical data [IR, energy-dispersive X-ray microanalysis, and CHN analysis] of compounds **3**−**6**, it is reasonable to propose for them the same structure as that found for **1**. Compounds **3**−**6** also adopt the LS state in the interval of 5−300 K.

Here we have shown a novel iron(II) microporous coordination polymer capable of sequestering water and organic molecules. The absorption/desorption of guest molecules takes place within seconds and is easily detectable because the guest-free and -loaded frameworks present distinct coloration and spin-state configurations. Inclusion in the framework of larger guest molecules and gases and the study of the guest-dependent SCO properties are currently ongoing work in our laboratory.

■ ASSOCIATED CONTENT

Ⓢ Supporting Information

Experimental section, crystallographic data in CIF format, TGA, TGA−MS, and PXRD patterns. This material is available free of charge via the Internet at http://pubs.acs.org.

■ AUTHOR INFORMATION

Corresponding Author

*E-mail: jose.a.real@uv.es.

Notes

The authors declare no competing financial interest.

■ ACKNOWLEDGMENTS

This work was supported by the Spanish Ministerio de Ciencia e Innovación (MICINN) and FEDER funds (Grant CTQ2010-18414) and the Generalitat Valenciana (Grants ACOMP2012/233 and PROMETEO2012/049). We acknowledge Dr. I. Boldog for helpful discussions. F.J.M.L. thanks MICINN for a predoctoral FPI fellowship.

■ REFERENCES

(1) (a) Kitagawa, S.; Kitaura, R.; Noro, S. *Angew. Chem., Int. Ed.* **2004**, *43*, 2334. (b) Férey, G. *Chem. Soc. Rev.* **2008**, *37*, 191.

(2) Dechambenoit, P.; Long, J. R. *Chem. Soc. Rev.* **2011**, *40*, 3249.

(3) Rocha, J.; Carlos, L. D.; Almeida Paz, F. A.; Ananias, D. *Chem. Soc. Rev.* **2011**, *40*, 926.

(4) (a) Avendano, C.; Zhang, Z.; Ota, A.; Zhao, H.; Dunbar, K. R. *Angew. Chem., Int. Ed.* **2011**, *50*, 6543. (b) Shimomura, S.; Kitagawa, S. *J. Mater. Chem.* **2011**, *21*, 5537.

(5) Shigematsu, A.; Yamada, T. H.; Kitagawa, H. *J. Am. Chem. Soc.* **2011**, *133*, 2034.

(6) (a) Gütlich, P., Goodwin, H. A., Eds. Spin Crossover in Transition Metal Compounds. *Topics in Current Chemistry*; Springer: Berlin, 2004; pp 233−235. (b) Real, J. A.; Gaspar, A. B.; Muñoz, M. C. *Dalton Trans.* **2005**, 2062. (c) Gaspar, A. B.; Ksenofontov, V.; Seredyuk, M.; Gütlich, P. *Coord. Chem. Rev.* **2005**, *249*, 2661. (d) Real, J. A.; Muñoz, M. C. *Coord. Chem. Rev.* **2011**, *255*, 2068.

(7) (a) Kahn, O.; Martinez, C. J. *Science* **1998**, *279*, 44. (b) Galet, A.; Gaspar, A. B.; Muñoz, M. C.; Bukin, G. V.; Levchenko, G.; Real, J. A. *Adv. Mater.* **2005**, *17*, 2949.

(8) Real, J. A.; Andrés, E.; Muñoz, M. C.; Julve, M.; Granier, T.; Bousseksou, A.; Varret, F. *Science* **1995**, *268*, 265.

(9) Halder, G. J.; Kepert, C. J.; Moubaraki, B.; Murray, K. S.; Cashion, J. D. *Science* **2002**, *298*, 1762.

(10) Neville, S. M.; Halder, G. J.; Chapman, K. W.; Duriska, M. B.; Southon, P. D.; Cashion, J. D.; Lètard, J. F.; Moubaraki, B.; Murray, K. S.; Kepert, C. J. *J. Am. Chem. Soc.* **2008**, *130*, 2869.

(11) (a) Niel, V.; Martinez-Agudo, J. M.; Muñoz, M. C.; Gaspar, A. B.; Real, J. A. *Inorg. Chem.* **2001**, *40*, 3838. (b) Ohba, M.; Yoneda, K.; Agustí, G.; Muñoz, M. C.; Gaspar, A. B.; Real, J. A.; Yamasaki, M.; Ando, H.; Nakao, Y.; Sakaki, S.; Kitagawa, S. *Angew. Chem., Int. Ed.* **2009**, *48*, 4767. (c) Southon, P. D.; Liu, L.; Fellows, E. A.; Price, D. J.; Halder, G. J.; Chapman, K. W.; Moubaraki, B.; Murray, K. S.; Létard, J. F.; Kepert, C. J. *J. Am. Chem. Soc.* **2009**, *131*, 10998.

(12) Agustí, G.; Ohtani, R.; Yoneda, K.; Gaspar, A. B.; Ohba, M.; Sánchez-Royo, J. F.; Muñoz, M. C.; Kitagawa, S.; Real, J. A. *Angew. Chem., Int. Ed.* **2009**, *48*, 8944.

(13) Ohtani, R.; Yoneda, K.; Furukawa, S.; Horike, N.; Kitagawa, S.; Gaspar, A. B.; Muñoz, M. C.; Real, J. A.; Ohba, M. *J. Am. Chem. Soc.* **2011**, *133*, 8600.

(14) Agustí, G.; Cobo, S.; Gaspar, A. B.; Molnár, G.; Ould Moussa, N.; Szilágyi, P. A.; Pálfi, V.; Vieu, C.; Muñoz, M. C.; Real, J. A.; Bousseksou, A. *Chem. Mater.* **2008**, *20*, 6721.

(15) Bartual-Murgui, C.; Ortega-Villar, N. A.; Shepherd, H. J.; Muñoz, M. C.; Molnar, G.; Salmon, L.; Bousseksou, A.; Real, J. A. *J. Mater. Chem.* **2011**, *21*, 7217.

(16) Muñoz Lara, F. J.; Gaspar, A. B.; Muñoz, M. C.; Arai, M.; Kitagawa, S.; Ohba, M.; Real, J. A. *Chem.—Eur. J.* **2012**, *18*, 8013.

(17) (a) Senchyk, G. A.; Lysenko, A. B.; Rusanov, E. B.; Chernega, A. N.; Krautscheid, H.; Domasevitch, K. V. *Inorg. Chim. Acta* **2009**, *362*, 4439. (b) Senchyk, G. A.; Lysenko, A. B.; Boldog, I.; Rusanov, E. B.; Chernega, A. N.; Krautscheid, H.; Domasevitch, K. V. *Dalton Trans.* **2012**, *41*, 8675.